A graphic element for the chapter header, consisting of a horizontal rounded rectangle with a blue border. The left portion is filled with a yellow-to-orange gradient, and the right portion is white. The text 'CHAPTER 7' is written in blue, with the '7' being significantly larger than the other characters.

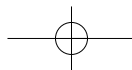
CHAPTER 7

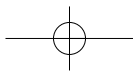
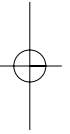
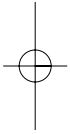
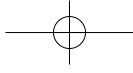
A registration mark consisting of a circle with a crosshair inside, used for alignment during printing.

**MODELLING DRUG RELEASE IN  
CARDIOVASCULAR ELUTING STENTS**

A registration mark consisting of a circle with a crosshair inside, used for alignment during printing.

***Grassi M, Grassi G, Pontrelli G, Teresi L.***





## Modelling drug release in cardiovascular eluting stents

### 7.1 INTRODUCTION

Endovascular stents are commonly implanted to improve or restore distal perfusion to the downstream tissues in patients with obstructive coronary diseases. Over the past few decades, implantation of drug-eluting stents (DES) following transluminal angioplasty has revealed as a well established technique for treating occlusions caused by the atherosclerotic plaques and to limit the so-called “in stent restenosis” process.

Although DES represent an important improvement in the management of arterial diseases, their long-term benefits and safety remain uncertain. Many factors are found to influence their performance, such as the geometry, the mechanical properties, its deployment, the drug delivery and the local fluid dynamics: much effort in modelling is currently addressed to a deeper understanding of the complex drug elution mechanism. As a matter of fact, mathematical modelling has emerged in recent years to investigate the mechanical response to stent placement and to simulate the delivery process. Even though a complete study needs a coupling with the blood flow and a thorough pharmacokinetics analysis, notwithstanding a simplified release model provides a deep insight into the complex physics and evidences the role played by the mass convection, diffusion phenomena and drug metabolism in the vascular wall, which are the basic concurrent phenomena involved in the drug release.

This chapter presents an overview about the technologies in DES which are applied and are being developed for the treatment of in stent restenosis. The first part describes the arterial wall anatomy and the pathological states of atherosclerosis and restenosis: this is crucial for understanding the environment where the drug delivery takes place (sect. 7.2). Due to a number of possible failures and long-term drawbacks, alternative approaches to drug release technology are currently suggested. One of these consists of the endoluminal gel paving (EGP) (sect. 7.3). In sect. 7.4, the classical and the alternative methodologies are compared through a mathematical model able to predict the drug distribution and its evolution in time over a cross-section of the wall. Though limited to an idealised configuration, the present model is shown to catch most of the relevant and combined aspects of the drug and fluid dynamics. By showing the relationship among the several variables and material parameters, it can be used to identify simple indexes or clinical indicators of biomedical significance and to optimise drug elution for a desired tissue concentration. Numerical simulations show that a bi-layer gel paving guarantees a uniform drug elution and a prolonged perfusion of the tissues and remains a promising and effective technique in drug delivery (sect. 7.5).

### 7.2 PHYSIOLOGY AND PATHOLOGY OF THE ARTERIAL WALL

**Arterial anatomy** The normal artery wall consists of three layers termed, from the inner to the outer, the intima, the media, and the adventitia, respectively (Figure 7.2.1). The intima is constituted by a continuous layer of endothelial cells (ECs) adherent to a layer of loose connective tissue named “inner elastic lamina”. Endothelial cells form a barrier that controls the entry of substances from the blood into the arterial wall and prevent clotting. Moreover, ECs can secrete substances that influence the contraction-relaxation of the subjacent vascular smooth muscle cells (VSMCs).

## CHAPTER 7 ●●●●

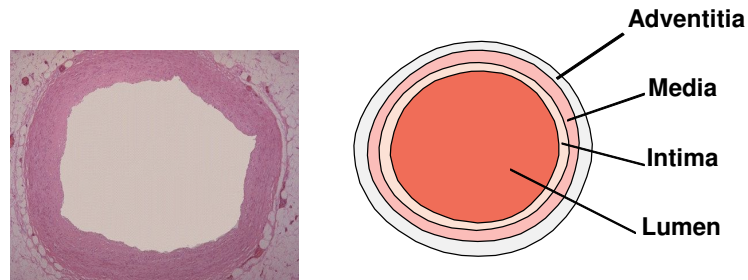


Figure 7.2.1 Anatomy of the three-layers arterial wall.

The media consists of only one cell type, the VSMCs organised in either a single layer (as in small muscular arteries) or in multiple lamellae (as in elastic arteries). The cells of the inner part of the media receive the nutrients from the vessel lumen while the cells of the outer part are nourished by small vessel termed *vasa-vasorum* which originate in the adventitia.

In the media, VSMC are surrounded by small amounts of collagen and elastic fibers which they produce together with other extra-cellular molecules. VSMCs are highly specialised cells whose principal function consists of the contraction and regulation of blood vessel tone-diameter, blood pressure, and blood flow distribution. VSMCs within adult blood vessels proliferate at an extremely low rate, exhibit very low synthetic activity, and express a unique repertoire of proteins required for the cell's contractile function [1]. However, unlike skeletal and cardiac muscle that are terminally differentiated, VSMCs can undergo rather profound and reversible changes in phenotype in response to changes in local environment. A classical example is represented by vascular injury, where the VSMCs dramatically increase their rate of proliferation, migration, and the capacity to produce different extra-cellular matrix molecules, in order to repair the vessel damage.

The adventitia, delimited from the media by a non continuous sheet of elastic tissue (external elastic lamina), consists of a loose mixture of collagen, elastic fibres, VSMCs, fibroblasts and contains *vasa vasorum* and nerves.

**Atherosclerosis** Arteriosclerosis represents a generic term indicating the thickening and hardening of the arterial wall, which is responsible for the majority of deaths in most westernised societies. One type of arteriosclerosis, defined atherosclerosis, is a disorder which involves larger arteries and which underlies most coronary and cerebro-vascular diseases.

Atherosclerosis can be considered a form of chronic inflammation [2]. This inflammatory process ultimately leads to the development of complex lesions, also defined plaques, that protrude into the arterial lumen. Plaque rupture and thrombosis result in acute clinical complications such as myocardial infarction and stroke, when the event occurs in coronary or cerebral arteries, respectively [1].

Although advanced atherosclerotic lesions can lead to ischemic symptoms as a result of progressive narrowing of the vessel lumen, acute cardiovascular events can also originate from plaque rupture. This exposes plaque lipids and tissue factor to blood components, initiating the coagulation cascade, platelet adherence thus leading to thrombosis and to a sudden vascular occlusion with the related ischemic symptoms [3].

**Artery restenosis and stenting** When atherosclerosis affects coronary arteries, symptoms such as angina pectoris and heart attack can occur. In order to re-vascularize stenotic coronary arteries, since 1979 it has been introduced the so called percutaneous transluminal coronary angioplasty

## Modelling drug release in cardiovascular eluting stents

(PTCA) [4]. This is a non-surgical method that has been shown to be safe and effective in comparisons with coronary artery bypass graft, a surgical approach used to circumvent artery stenosis.

PTCA procedure (Figure 7.2.2) involves: 1) advancing a balloon catheter to an area of coronary narrowing, 2) inflating the balloon, 3) retrieving the catheter following balloon deflation.

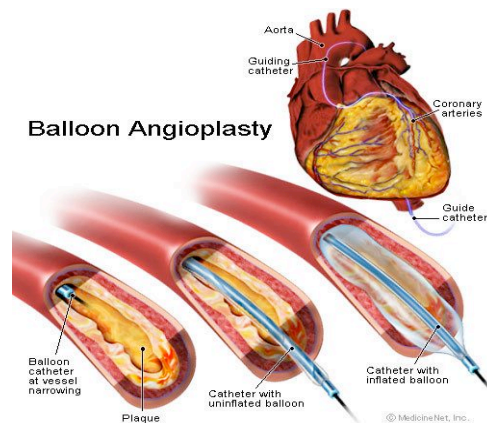


Figure 7.2.2 PTCA procedure (from [www.medicinenet.com/images/illustrations/balloon\\_angio.jpg](http://www.medicinenet.com/images/illustrations/balloon_angio.jpg)).

However, PTCA has been shown to induce the development of symptomatic re-occlusion (restenosis) caused by early elastic recoil, intimal thickening, late constricting remodelling of the vessel [5] and formation of mural thrombus in about 30-50% of treated patients [6].

To try to overcome the PTCA related problems, the expansion of the balloon during angioplasty has been associated with the deployment of a stent. This is an expandable metal - or polymeric - tubular mesh (see also next section) firstly developed in 1987 (Figure 7.2.3) [7]. The deployment of the stents has significantly reduced the rates of early elastic recoil and late constructive remodelling of the vessel reducing restenosis rate down to 20-30% [8]. The partial success of the stents is due to the induction of the intimal thickening (in-stent restenosis, ISR), a phenomenon particularly evident in small calibre vessels [5] and characterised by an exuberant proliferation of VSMCs. Clinical ISR produces recurrent angina or evidence of myocardial ischemia.

## CHAPTER 7

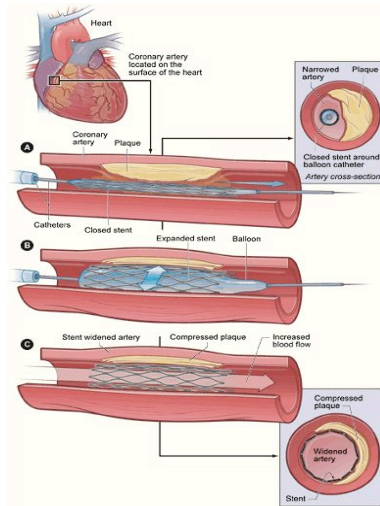


Figure 7.2.3 Endovascular implantation of a bare metal stent (from: [www.nhlbi.nih.gov/health/dci/images/stent\\_lowres.gif](http://www.nhlbi.nih.gov/health/dci/images/stent_lowres.gif)).

With the aim to overcome the excessive VSMC proliferation observed after bare metal stent implantation, devices able to locally deliver anti-proliferative drugs have been developed (Figure 7.3.1). Currently, more than 85% of all coronary interventions in the United States are performed with drug-eluting stents (DES).

However, some concerns related to the use of DES are now emerging [9-11]. In this regard, recent indications suggest that many drawbacks may be eliminated with a better understanding the biology of ISR [12], by focusing on the development of more appropriated stent both with respect to novel drug delivery systems and to the geometrical/mechanical design, a fact which can substantially affect blood flow and thus ISR occurrence. These issues will be discussed in the next section.

### 7.3 THE STENTING TECHNOLOGY

Although biological and individual factors can influence the clinical results, successful outcomes of stent implantations are also strictly related to design parameters such as stent building material, surface properties and geometrical characteristics [13].

Coronary stents structure (named strut) is generally made up by metals or polymers. Metallic stent struts can be constituted by stainless steel, Nitinol, an alloy of nickel and titanium, or tantalum. Whereas stainless steel, occasionally, can show thrombogenicity problems, Nitinol seems to overcome these problems even if this aspect is still under debate. The main advantage in using Nitinol relies on its high biocompatibility and shape memory. Finally, tantalum shows a good radiopacity, an important characteristic for the easy stent positioning. The employment of polymeric stent struts in place of metal ones is suggested by the fact that, by a proper selection of polymeric

## Modelling drug release in cardiovascular eluting stents

chains, a very good biocompatibility can be met. Polymeric stents can be subdivided into two classes: bio-stable and bio-degradable. While the first act as metallic stents and thus remain in situ forever without undergoing structural modifications, the second ones exert their action over a limited period of time and then disappear due to degradation into a-toxic compounds. Obviously, building material greatly contributes to the determination of stent radial resistance, a fundamental characteristic required to hinder artery wall early elastic recoil. While, in general, metallic stents ensure a good radial resistance, polymeric ones are characterised by poor mechanical properties.

As the successful performance of a stent can depend on its surface properties, many attempts of surface improving have been made. Accordingly, the stent surface is made as smooth as possible to avoid any possible inflammation process induced by a rough surface. Metallic stents undergo electropolishing in order to eliminate undesired contaminant that can favour the restenotic process. Alternatively, stent surface can be coated by a proper film that guarantees the desired, uniform, surface characteristics. Gold, showing reduced thrombogenicity in preclinical studies and being biocompatible and radiopaque, has been successfully used as stent coating material. Silicon carbide, a semiconductor material, has been used as stent coating in virtue of its low thrombogenic and inflammatory characteristics. In addition, the idea of a polymeric coating has been considered and different polymers such as polyurethane and polytetrafluoroethane yielded interesting results. Of course, other attempts have been undertaken to make stent surface more biocompatible. Among them, we mention the approaches for grafting surfaces with water-soluble polymers, such as heparin [14], phosphorylcholine- containing polymers [15], fibrin [16], albumin, poly(ethylene oxide) [17,18], and to deliver anti-thrombogenic agents from the surface [19].

Finally, a correct design must also account for stent geometrical characteristics, the most important of which are: length, diameter, strut thickness and mesh shape. If the stent diameter (after in situ expansion) and length (usually spanning from 10 to 40 mm) are dictated by physiological and pathological factors, the remaining two are at the designer disposal. Typically, strut thicknesses

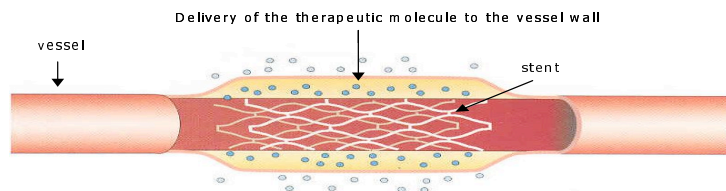


Figure 7.3.1 Mechanism of a drug-eluting stent.

ensuring satisfactory mechanical properties in metal stents span from 50 to 150 $\mu$ m [13]. In principle, the thinner the strut is, the better the stent works. Indeed, pressure drop per unit length and maximum wall shear stress decrease with strut thickness [20]. In addition, a thin strut usually prevents the formation of very low blood velocity fields, responsible for the deposition of different substances that can originate a new plaque. The issue of strut thickness is made more subtle by the nature of the plaque itself. Indeed, whereas in soft plaques the stent can be completely embedded in the wall-plaque structure, in strong (calcified) plaques it can completely protrude into the lumen. The definition of the best mesh shape is an art rather than science. Indeed, this problem is very hard and can be matched only when considering the interaction with blood flow. As a matter of fact, some shapes induce the formation of very low velocity fields more easily than others. Notably, Comel found that an important design parameter, strictly connected to the strut geometry, is the

CHAPTER 7 

stent void fraction  $\phi$  [20]. This is defined as the ratio between the stent surface in contact with the vessel wall and the whole surface of the stented vessel (typically,  $\phi$  ranges between 0.6 and 0.8). It turns out that pressure drop per unit length and maximum wall shear stress depends on  $\phi$  rather than on mesh shape. On the other way around, the tendency to yield a low velocity pattern is essentially dependent on the mesh geometry.

**Drug-eluting stents** Despite efficiently counteracting early elastic recoil and late constructive remodelling, stent implantation can cause injury to the blood vessel and this leads to neointimal thickening (ISR). To overcome this inconvenience, the elective treatment is the implantation of DES. This consists of one or more biocompatible polymeric coatings surrounding stent strut and containing the therapeutic agent to be delivered (Figure 7.3.1).

Typically, drug release rate can be controlled by physical or chemical mechanisms [21]. Physical mechanisms comprehend drug diffusion through the polymeric coating, polymeric coating dissolution/degradation, osmotic pressure, or exchange of ionised drugs. On the other hand, chemical mechanisms rely on the enzymatic breaking of the covalent bonds connecting drug molecules to the delivery vehicle, such as polymer chains. As chemical mechanisms require the modification of drug molecules for grafting to the delivery vehicle, physical mechanisms are more popular. In addition, adopting physical mechanisms, drug release rate can be controlled acting on simple design parameters such as coating thickness, drug diffusivity inside the coating, drug loading configuration (*matrix configuration*: drug dispersed in the coating; *reservoir configuration*: drug contained in proper depots realised in the stent strut and separated from the release environment by the coating) and the possibility of considering multilayered coatings where each layer shows different characteristics and/or drug loading. However, it is worth noting that the coating must exhibit sufficient elastic properties in order to avoid breaking and fracturing upon stent expansion. Therefore the selection of the proper coating is of paramount importance for the clinical success of DES technology. For example, the diffusion based TAXUS stent (Boston Scientific) employs a one layer triblock copolymer for the controlled release of Paclitaxel [22]. The diffusion based Cypher stent (Cordis Corp.), instead, uses a two layers coating [23]. The inner coating (basecoat) consists of a mixture of poly(ethylene-co-vinyl acetate), poly(n-butyl methacrylate) and sirolimus (drug) in a drug /polymer ratio equal to 0.5. The outer coating (topcoat) is made up by a thin layer of poly(n-butyl methacrylate). Usually, dissolution or degradation based stents employ slow dissolving water-soluble polymers or slow degrading hydrophobic polymers by hydrolysis. For example, in the Conor stent (Conor Medsystems) the holes present on the strut are filled with a biodegradable polymeric matrix made of poly(lactide-co-glycolide) containing paclitaxel. Drug release rate can be easily controlled acting on polymer degradation kinetics, depending on polymer molecular weight and on lactic/glycolic acid ratio [24]. Ion exchange based DESs are used for the controlled delivery of charged drugs such as DNA and RNA. The BiodivYsio stent, a stainless steel metal stent is coated with a copolymer of methacryloylphosphorylcholine and lauryl methacrylate [15]. Negatively charged drugs adhere to the positively charged polymeric coating and can be released due to replacement by negatively charged ions present in the body. In virtue of the multiple electrostatic interactions, DNA release is slow.

Unfortunately, recent studies evidence that existing DES are far from representing the final solution to the ISR problem [25-27]. Indeed, their use is connected to a high incidence of late thrombosis (due to an incomplete endotelisation of the stented zone) in comparison with uncoated stents. Up to now, the reasons for this behaviour are not clear. It could be argued that as only two drugs (sirolimus and paclitaxel) have been approved for human trials, DES failure could be attributed to an extremely aggressive action of these two drugs. Nevertheless, other contrasting opinions exist and alternative approaches for drug delivery strategies are now suggested.

**Gel paved stents** Among the therapeutic agents that could be used, nucleic acid based drugs (NABD) have been proved to hinder VSMCs exuberant proliferation by suppressing the expression



## Modelling drug release in cardiovascular eluting stents

of relevant cell cycle promoting genes [28,29]. The fragile nature and low cellular transfection attitude impose their complexation with proper delivery agents in order to make this approach effective and reliable from the therapeutic point of view. For example, fat substances such as liposomes and polycations have been successfully considered [30].

The dimensions and the physico-chemical characteristics of NABD-delivery agent complexes make their release from traditional DES problematic and alternative solutions are considered. The endoluminal gel paving technique (EGP) [31] together with the implantation of a bare metal stent seems to be an effective and promising approach (Figure 7.3.2). EGP consists in the catheter application of biocompatible polymer solutions over the endoluminal vessel surface followed by in situ polymerisation or crosslinking. To this purpose, several catheters have been designed and their details vary according to the rheological, chemical and physical properties of polymer solutions to be inserted. For example, for thermoreversible systems, a modified dual balloon catheter or a dispatch catheter can be used [32]. The modified dual balloon catheter consists of two occlusion balloons (proximal and distal) with an interposed third expanding balloon ensuring maintenance of a central lumen while an endoluminal gel tube forms between vessel wall and the third balloon. In order to avoid unfavourable pressure drop across the paved zone and too high wall shear stress, gel thickness should not exceed a given threshold (typically, 200 $\mu$ m with an artery diameter of 3mm [20]). Indeed, high wall shear stress can cause premature gel layer erosion.

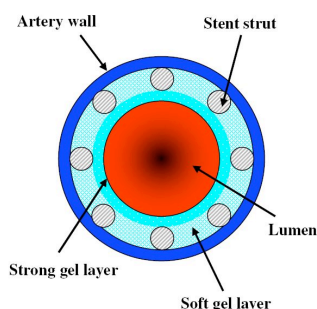


Figure 7.3.2 Schematic cross-section of a stented and gel paved artery (figure not in scale).

The potential advantages of the gel paving-stent technique are an easy and safe complex loading within the gel matrix and the opportunity of creating a physical barrier between the damaged artery wall and the overflowing thrombogenic and inflammatory elements present in the blood stream [33]. The success of this technology also depends on the materials adopted for gel formation. For example, Grassi and co-workers [30] consider a polymeric blend made up by Pluronic F127 [34] and alginate (Protanal 10/60) [35]. PF127 is a synthetic block copolymer that shows reverse thermo-responsive properties in aqueous solutions (low viscosity solution at room temperature and gel behaviour at higher temperature). This property makes PF127 very attractive as it can be easily combined with the NABD-delivery agent complexes by simple mixing at temperature around 4-8°C. Alginates are linear polymers that, in the presence of an aqueous solution containing bivalent cations, form temperature-insensitive hard gels. Accordingly, gel formation follows a two steps mechanism leading to a two-layer gel. While the physiological temperature allows solution gelation due to PF127 transition, the subsequent exposition of the inner gel surface to a solution containing bivalent cations causes the gelation of the alginate component. The fast exposition to bivalent

CHAPTER 7 

cations prevents from a complete film gelation thus leaving an outer soft layer made up by gelled pluronic, not crosslinked alginate and NABD-delivery agent complexes and an inner one composed by gelled alginate, PF127 and NABD-delivery agent. The inner hard layer is thought to resist to the blood flow erosion, protecting the soft layer which can release the NABD-delivery agent complexes to the arterial wall where VSMCs, the target cells, reside. The strong cross-linking degree of the hard layer prevents from NABD/delivery agent release in the systemic circulation.

## 7.4 MATHEMATICAL MODELLING OF DRUG ELUTION

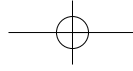
A fundamental prerequisite for the realisation of a new drug delivery system is the knowledge of its release characteristics. To this aim, a theoretical study aimed to evaluate the relative importance of the design parameters needs to be carried out [36]. Moreover, the comparison with traditional similar delivery systems can be useful to make clear the advantages and the drawbacks of the novel approach. Finally, the theoretical approach becomes more and more important when, as in the present case, the experimental set up remains uncertain. Accordingly, this section is aimed to develop a proper mathematical model for drug release in DES and EGP.

Several efforts have been made to model drug delivery from DES (see [37-38] and references therein), but much less attention was paid to gel paved systems. As a preliminary step of modelling, the physiological framework into which the drug release takes place has to be identified.

**Biological framework** Let us consider an ideal drug molecule that, from the coating, has to cross several layers before spreading in the artery wall. Firstly, apart from the unavoidable diffusion in the coating itself, it partitions from the delivery system to the intima. Here, its dynamics is essentially due to diffusion, induced by the existing concentration gradient, and convection, due to a radial hydrostatic pressure gradient between lumen and artery wall [39]. In order to reach the media, the drug molecule must partition from the intima to the internal elastic lamina and then to the media. Again, diffusion and convection govern its motion even though drug binding to proteins and metabolism can affect it. While drug binding to proteins is reversible, metabolism (here meant as cellular internalisation) is irreversible and leads to drug disappearing. In this context, arterial wall can be schematised as an inter-channelled structure where free drug molecules, moving in the fluid filling the channels, progressively bind to proteins and are metabolised [40]. Again, drug molecule transport to adventitia requires two further steps: media – external elastic lamina – adventitia. Once in the adventitia, the molecule is swept out by *vasa vasorum*, and lymphatic drainage and lost into connective tissues. This mechanistic description of drug transport coupled with the intrinsic three-dimension character of drug transport in the artery wall clearly underlines the complexity of the release mechanism. Furthermore, the relative importance of the various sub-phenomena discussed (diffusion, convection, partitioning and binding) depends on drug characteristics (molecular weight, charge, hydrophilic or hydrophobic nature), arterial pathological conditions and geometrical features of the release device. As a complete and detailed description of all the sub-phenomena lead to very complex models and need a high number of variables and parameters, many different levels of simplifications in modelling have been made [41].

**Conventional DES** Let us consider a stent coated by a thin layer of gel containing a drug and embedded into the arterial wall, as illustrated in Figure 7.4.1. The complex multi-layered structure of the arterial wall has been disregarded and a homogeneous material with averaged properties has been considered for simplicity (*fluid-wall* model) [41]. Both the coating and the arterial wall are treated as porous media.

For the sake of simplicity, we restrict our study to a simplified 2D model and we assume the stent structure to be regular, having the width and the spacing of the meshes constant. As



## Modelling drug release in cardiovascular eluting stents

consequence, it is sufficient to consider a cross section of the wall and a slice of it containing a single strut  $\Sigma$  embedded into the wall at distance  $s$  from the endothelium. In this idealised case, the full section of the stented artery is obtained from such a portion by circular symmetry and periodicity. Moreover, being the wall thickness very small with respect to the arterial radius, a cartesian coordinate system  $(x,y)$  is used on the tangential plane (Figure 7.4.1). We denote by  $l$  (resp.  $d$ ) the width (resp. the thickness) of this rectangular portion of the wall, by  $L_x$  (resp.  $L_y$ ) the half-length (resp. the thickness) of the strut embedded in it, and by  $s$  the penetration depth (the coating is supposed to be a thin layer around the strut of uniform thickness  $h_c$ ). The strut represents a mechanical obstacle to the drug release, while the wall and the coating constitute a coupled two-layered system where mass dynamics takes place. Such interfaced domains are denoted respectively by  $\Sigma = [0, L_x] \times [s, s+L_y]$  (*strut*),  $\Omega_c$  (*coating*) and  $\Omega_w = [0, l] \times [0, d] \setminus (\Omega_c \cup \Sigma)$  (*wall*)<sup>1</sup> (Figure 7.4.1). Here, and throughout this chapter, a mass volume-averaged concentration  $c(x,t)$  ( $\mu\text{g}/\text{cm}^3$ ) is considered and a subindex is used for denoting the correspondent medium.

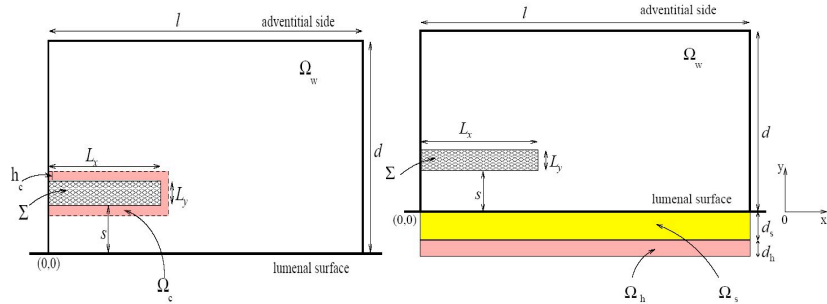


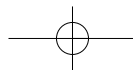
Figure 7.4.1 Two configurations for arterial drug delivery: traditional DES (left) and endoluminal gel paving (right). The pattern refers to a single embedded half-strut and repeats symmetrically on the left and on the right sides to complete a circular cross section (figure elements are not in scale, but share the same dimensions and parameters).

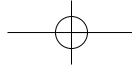
At the beginning, the drug is contained only in the coating  $\Omega_c$  and it is uniformly distributed at a maximum concentration  $C_c$  and, subsequently diffused into the wall. Thus, the dynamics of the drug in the coating is described by the following diffusion equation<sup>2</sup>:

$$\begin{aligned}
 \frac{\partial c_c}{\partial t} - \nabla \cdot (D_c \nabla c_c) &= 0 && \text{in } \Omega_c \\
 \nabla c_c \cdot \mathbf{n}_c &= 0 && \text{on } \partial\Omega_c|_{x=0} \\
 \nabla c_c \cdot \mathbf{n}_c &= 0 \quad (\text{impermeability}) && \text{on } \partial\Omega_c|_{x=0} \cap \partial\Sigma \\
 c_c &= C_c && \text{at } t = 0
 \end{aligned} \tag{7.4.1}$$

Let us now consider the drug dynamics in the wall. Here mass transfer is not governed by diffusion only, but convection due to the filtration velocity of the plasma results equally important

<sup>1</sup> In the chapter, subscript c (resp. w) refers to the coating (resp. to the wall).  
<sup>2</sup>  $D$  denotes the drug diffusivity and  $\mathbf{n}$  the normal external to the medium.





CHAPTER 7 ●●●●

and a transport term is added. Furthermore we account for a metabolic process (due to drug binding or chemical reaction) and a linear mass consumption is assumed. At adventitial side ( $y \rightarrow d$ ), being  $d \cdot s \gg L_y$ , the concentration  $c_w$  at  $y = d$  does not change with time and hence it remains equal to its initial value, namely zero. Similarly,  $c_w = 0$  at  $y = 0$  because of the wash out of the blood stream. Therefore, a fraction of drug is lost in the tissues adjacent to the adventitia and a fraction dispersed in the lumen. Thus, we have the following convection-diffusion-reaction problem:

$$\begin{aligned} \frac{\partial c_w}{\partial t} + \nabla \cdot (\gamma \mathbf{U}_w \cdot c_w - D_w \nabla c_w) + \beta c_w &= 0 && \text{in } \Omega_w \\ c_w = 0 \quad (\text{washout or large distance}) &&& \text{on } \partial\Omega_w|_{y=0} \cup \partial\Omega_w|_{y=d} \\ \nabla c_w \cdot \mathbf{n}_w = 0 \quad (\text{symmetry}) &&& \text{on } \partial\Omega_w|_{x=0} \cup \partial\Omega_w|_{x=l} \\ c_w = 0 &&& \text{at } t = 0 \end{aligned} \quad (7.4.2)$$

where  $\mathbf{U}_w$  is a wall volume-averaged plasma filtration velocity,  $\gamma$  an advection parameter,  $\beta > 0$  a consumption rate coefficient.

The previous system of eqns. (7.4.1)- (7.4.2) is completed by suitable conditions at the coating-wall interface. One of them is obtained by imposing conservation of the mass flux:

$$D_c \nabla c_c \cdot \mathbf{n}_c = D_w \nabla c_w \cdot \mathbf{n}_w \quad \text{on } \partial\Omega_c \cap \partial\Omega_w \quad (7.4.3)$$

Let  $\Pi$  (cm/s) be the permeability of the topcoat located at the coating/wall interface  $x = 0$ . A continuous mass flux passes through it orthogonally to the coating film with a possible concentration jump. In the present case, the mass transfer through the topcoat can be described using the second Kedem-Katchalsky equation [42].

Thus, the continuous flux of mass passing across the membrane orthogonally to the coating is expressed by:

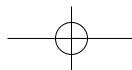
$$-D_c \nabla c_c \cdot \mathbf{n}_c = -D_w \nabla c_w \cdot \mathbf{n}_w = \Pi(c'_c - c'_w) \quad (7.4.4)$$

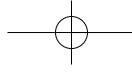
with  $c'$  the fluid-phase concentration. This is related to the volume-averaged concentration  $c$  through the formula  $c' = c/k\varepsilon$ , where  $\varepsilon$  is the porosity and  $k$  is the partition coefficient [40]. Eqns (7.4.1)-(7.4.4) apply to all the three sides of the coating-wall interface (dashed lines in Figure 7.4.1a).

**Gel paved stent** In the light of what discussed in section 7.3, the gel paved stent configuration can be schematised as in Figure 7.4.1b, where subscript  $s$  (resp.  $h$ ) refers to soft gel with domain  $\Omega_s$  and thickness  $d_s$ , (resp. hard gel with domain  $\Omega_h$  and thickness  $d_h$ ).

Differently than in the case of traditional DES, the double gel layer prevents convection across the arterial wall, and the motion equation (7.4.2) now simplifies as:

$$\frac{\partial c_w}{\partial t} + \nabla \cdot (-D_w \nabla c_w) + \beta c_w = 0 \quad \text{in } \Omega_w \quad (7.4.5)$$





## Modelling drug release in cardiovascular eluting stents

Due to the absence of metabolic activity in both the soft and hard gel layer, the transport equation pertaining to these domains reduces to the simple diffusion equation:

$$\frac{\partial c_i}{\partial t} + \nabla \cdot (-D_i \nabla c_i) = 0 \quad \text{in } \Omega_i \quad i = h, s \quad (7.4.6)$$

Eqs. (7.4.5) and (7.4.6) are supplemented by the following boundary and initial conditions:

*Boundary conditions along horizontal sides:*

$$\begin{aligned} c_h &= 0 && \text{on } \partial\Omega_h|_{y=-d_h-d_s} \\ D_h \nabla c_h \cdot \mathbf{n}_h &= D_s \nabla c_s \cdot \mathbf{n}_s && \frac{c_h}{c_s} = k_{hs} \quad \text{on } \partial\Omega_h \cap \partial\Omega_s \\ D_s \nabla c_s \cdot \mathbf{n}_s &= D_w \nabla c_w \cdot \mathbf{n}_w && \frac{c_s}{c_w} = k_{sw} \quad \text{on } \partial\Omega_s \cap \partial\Omega_w \\ \nabla c_w \cdot \mathbf{n}_w &= 0 \quad (\text{impermeability}) && \text{on } \partial\Omega_w \cap \partial\Sigma \\ c_w &= 0 \quad (\text{large distance}) && \text{on } \partial\Omega_w|_{y=d} \end{aligned} \quad (7.4.7)$$

*Boundary conditions along vertical sides:*

$$\nabla c_i \cdot \mathbf{n}_i = 0 \quad (\text{symmetry}) \quad \text{on } \partial\Omega_i|_{x=0} \cup \partial\Omega_i|_{x=l} \quad i = h, s, w \quad (7.4.8)$$

*Initial conditions:*

$$c_w = 0 \quad c_s = C_s \quad c_h = C_h \quad \text{at } t = 0 \quad (7.4.9)$$

where  $k_{sh}$  and  $k_{sw}$  are, respectively, the hard/soft gel and the soft gel/wall partition coefficients.

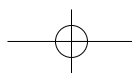
### 7.5 NUMERICAL SIMULATIONS AND COMPARATIVE RESULTS

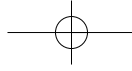
We are interested in studying the variation of the concentration field in the wall with the geometrical parameters such as the penetration depth  $s$  that measures the stent embedding degree, or the mesh length  $L_x$  directly related to the void fraction. Our aim is to compare the mass release in the two configurations of conventional DES (case i) and EGP (case ii). Comparison is difficult because much of the parameters and the materials are intrinsically related to the specific methodology. However, the following physical values are fixed for computational experiments in both configurations (Figure 7.4.1):

$$d = 0.08 \text{ cm} \quad l = 0.4 \text{ cm} \quad L_y = 0.005 \text{ cm} \quad D_w = 7 \cdot 10^{-8} \text{ cm}^2/\text{s}$$

In both cases, all concentrations (considered as averaged mass per area) are nondimensionalised with respect to their initial values ( $c \rightarrow c/C_c$  in the case (i), and  $c \rightarrow c/C_h$  ( $C_s=C_h$ ) in case (ii)). For the conventional stent, the following constants are considered:

$$h_c = 5 \mu\text{m} \quad \Pi = 10^{-6} \text{ cm/s} \quad D_c = 10^{-10} \text{ cm}^2/\text{s}$$





CHAPTER 7 ●●●●

$$k_c = 1 \quad k_w = 1 \quad \varepsilon_c = 0.1 \quad \varepsilon_w = 0.61$$

They reflect typical scales in DES and are in agreement with experimental evidence and data in literature for the coronary arterial wall and heparin drug in the coating layer [40,43].

A short analysis of fluid mechanics shows that, if the thickening of gel layer allows higher drug doses and a prolonged release, on the other hand, it implies an unacceptable high pressure drop. A reasonable compromise suggests setting the gel layer thickness around 220µm. In addition, the optimal partition between  $d_s$  and  $d_h$  is related to both drug delivery and mechanical properties. As a matter of fact, while a thinner  $d_h$  would reflect in a too weak protection against blood erosive action, a thicker  $d_h$  would considerably limit drug diffusion towards arterial wall as drug mobility in the hard gel is very low. According to such analysis, a ratio  $d_h/d_s \cong 0.1$  is suggested and simulations for EGP system are carried out with the following gel layer thickness:

$$d_s = 200 \mu m \quad d_h = 20 \mu m$$

and with physical parameters:

$$D_s = 10^{-9} cm^2/s \quad D_h = 10^{-12} cm^2/s \quad k_{sh} = 1 \quad k_{sw} = 1$$

The problem of mass release apparently depends on a large number of parameters, each of them run in a finite range, and there is a variety of different limiting cases. As a matter of fact, they cannot be chosen independently from each other, but they are related by some compatibility condition to give rise a realistic output. A sensitivity analysis is carried out at varying void fraction  $l-L_x$  ( $L_x = 0.05 \div 0.1 cm$ ) and penetration depth ( $s = d/10 \div 9d/10$ ). Moreover, the wall filtration velocity ( $U_w \approx 10^{-6} cm/s$ ) is inhibited by the hard gel barrier in case (ii) and acts as an unfavorable factor in case (i): therefore it is not considered for comparative purposes. Similarly  $\beta = 0$ , since the metabolic process does not influence the comparison and the relative performance of the two cases.

The numerical problem has been solved by finite element method using COMSOL multiphysics package. The spatial domain has been discretised by a not uniform triangular mesh (having a number of elements  $\approx 3200$  in case (i) and  $\approx 2600$  in case (ii)), with second order Lagrangian polynomial as shape functions; a Runge-Kutta time integration scheme with adaptive time step has been chosen (minimum  $\Delta t \approx 10^{-2}$ ).

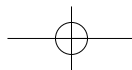
Simulations of drug release are carried out for a period of time up to 5 days (120 hours): results indicate that concentration level in the wall increase up to a maximum level and then decrease exponentially to zero. The release time grows tremendously in EGP case.

The drug mass in the wall is computed as:  $M(t) = \int_{\Omega_w} c_w(x, y, t) dx dy$  and is referred to the total

$$\text{initial mass: } M(0) = \int_{\Omega_c} c_{tot}(x, y, 0) dx dy = |\Omega_c| \quad (\text{case i}) \quad \text{and} \quad M(0) = \int_{\Omega_s \cup \Omega_h} c_{tot}(x, y, 0) dx dy = |\Omega_s + \Omega_h|$$

(case ii), being  $c_{tot}(x, y, 0) = 1$ .

Several test cases are carried out by varying the penetration depth ( $s$ ) and mesh length ( $L_x$ ). In Figure 7.5.1 the ratios  $\frac{M(t)}{M(0)}$  are reported for (i) and (ii). Results show that mass in the wall first increase up to a maximum value and then, owing to the absorption at  $y = 0$  and at  $y = d$ , decay exponentially in a finite time. It is shown that the mass elution is slowed down up to 10 times in the case (ii). The most favourable case is obtained when both  $s$  and  $L_x$  are kept high. In the traditional DES (see Figure 7.5.1, dashed line), a negligible difference is found with  $s$  and  $L_x$ , either in the emptying time and in the peak value, while a tremendous increase of mass release is found in EGP



## Modelling drug release in cardiovascular eluting stents

methodology. Moreover, the peak for M is much higher and occurs later in the latter case. A larger value of the peak and a slower drug elution is obtained by increasing  $s$  or  $L_x$  [44].

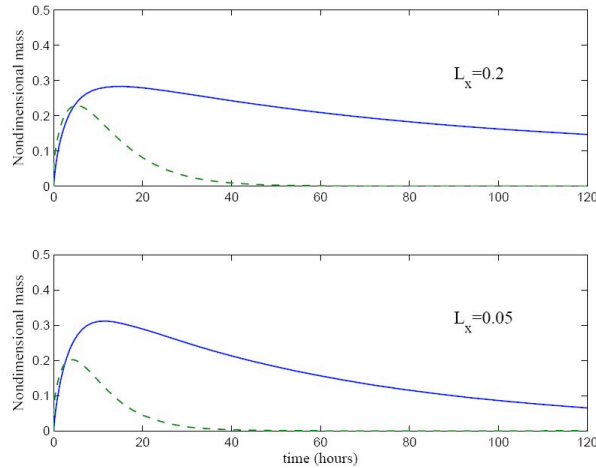


Figure 7.5.1 Nondimensional mass as function of time in case i (dashed line) and ii (continuous line), for a penetration depth of  $s=d/10$ . Plots above and below refer to different strut mesh size  $L_x$ . Differently than traditional DES, the EGP methodology turns out to be more sensitive to geometrical parameters.

Results of drug release in DES are compared with those obtained in an even simpler 1D model [38]. The discrepancy of both concentration field and the mass along a transversal direction is less of 10%. On the other hand, results from this preliminary study indicate that EGP guarantees a more localised drug elution and reduce systemic losses. In other words, it seems to enable a more *controlled* and *effective* drug release than the traditional DES for the treatment of atherosclerosis and restenosis. More sensitive to the geometrical factors, and tuned in optimal way, EGP can be used to design novel efficient drug delivery systems and to improve therapeutic protocols. EGP can be used to enhance the reliability and effectiveness of gel paving based techniques. In addition, the possibility of modulating release rate acting on gel properties regardless stent characteristics, makes it very versatile and suitable for future improvements related to the discovery of new gels formulation.

Finally, should the gel be paved after stent implantation, it is not subject to the considerable stretching present in the polymeric coating of standard DES. These considerations and the recently raised problems connected with the use of traditional DES, open new perspectives and encourage further investigations of unconventional approaches of drug delivery such as those based on the presented EGP technology.

## CHAPTER 7

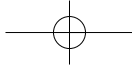
**References**

1. Owens GK, Kumar MS, Wamhoff BR. Molecular regulation of vascular smooth muscle cell differentiation in development and disease. *Physiol. Rev.* 2004; 84: 767–801.
2. Ross R. Atherosclerosis: an inflammatory disease. *N. Engl. J. Med.* 1999; 340: 115–126.
3. Fiotti N, Altamura N, Fiscaro M, Carraro N, Uxa L, Grassi G, Torelli L, Gobbato R, Guarnieri G, Baxter BT, Giansante C. MMP-9 microsatellite polymorphism and susceptibility to carotid arteries atherosclerosis. *Arterioscl. Thromb. Vasc. Biol.* 2006; 26: 1330–1336.
4. Gruntzig AR, Senning A, Siegenthaler WE. Nonoperative dilatation of coronary-artery stenosis: percutaneous transluminal coronary angioplasty. *N. Engl. J. Med.* 1979; 301: 61–68.
5. Ruygrok PN, Webster MW, Ardill JJ, Chan CC, Mak KH, Meredith IT, Stewart JT, Ormiston JA, Price S. Vessel caliber and restenosis: a prospective clinical and angiographic study of NIR stent deployment in small and large coronary arteries in the same patient. *Catheter Cardio. Interv.* 2003; 59: 165–171.
6. Califf RM. Restenosis: the cost to society. *Am. Heart J.* 1995; 130: 680–684.
7. Sigwart U, Puel J, Mirkovitch V, Joffre F, Kappenberger L. Intravascular stents to prevent occlusion and restenosis after transluminal angioplasty. *N. Engl. J. Med.* 1987; 316: 701–706.
8. Serruys PW, de Jaegere P, Kiemeneij F, Macaya C, Rutsch W, Heyndrickx G, Emanuelsson H, Marco J, Legrand V, Materne P. A comparison of balloon-expandable-stent implantation with balloon angioplasty in patients with coronary artery disease. Benestent Study Group. *N. Engl. J. Med.* 1994; 331: 489–495.
9. Tung R, Kaul S, Diamond GA, Shah PK. Narrative review: drug-eluting stents for the management of restenosis: a critical appraisal of the evidence. *Ann. Int. Med.* 2006; 144:913–919.
10. Serruys PW, Daemen J. Are drug-eluting stents associated with a higher rate of late thrombosis than bare metal stents? Late stent thrombosis: a nuisance in both bare metal and drug-eluting stents. *Circulation.* 2007; 115: 1433–1439.
11. W.H. Maisel, Unanswered Questions: drug-eluting stents and the risk of late thrombosis, *New Eng. J. Med.* 2007; 356: 981–984.
12. Luscher TF, Steffel J, Eberli FR, Joner M, Nakazawa G, Tanner FC, Virmani R. Drug-eluting stent and coronary thrombosis: biological mechanisms and clinical implications. *Circulation.* 2007; 115: 1051–1058.
13. Hara H, Nakamura M, Palmaz JC, Schwartz RS. Role of stent design and coatings on restenosis and thrombosis. *Adv. Drug Deliv. Rev.* 2006; 58 (2): 377–386.
14. Hardhammar PA, Beusekom HMMV, Emanuelsson HU, Hofma SH, Albertsson PA, Verdouw P, Boersma E, Serruys PW, Reduction in thrombotic events with heparin-coated Palmaz–Schatz stents in normal porcine coronary arteries. *Circulation.* 1996; 90: 423–430.
15. Whelan DM, Giessen WJVD, Krabbendam SC, Vliet EAV, Verdouw PD, Serruys PW, Beusekom HMM. Biocompatibility of phosphorylcholine coated stents in normal porcine coronary arteries. *Heart Drug.* 2000; 83: 338–345.
16. Holmes DR, Camrud AR, Jorgenson MA, Edwards WD, Schwartz RS. Polymeric stenting in the porcine coronary artery model: differential outcome of exogenous fibrin sleeves versus polyurethane-coated stents. *J. Am. Coll. Cardiol.* 1994; 24: 524–531.
17. Park K, Shim HS, Dewanjee MK, Eigler NL. In vitro and in vivo studies of PEO-grafted blood-contacting cardiovascular prostheses. *J. Biomater. Sci., Polym. Ed.* 2000; 11: 1121–1134.
18. Mcpherson TB, Shim HS, K. Park K. Grafting of PEO to glass, nitinol, and pyrolytic carbon surfaces by gamma irradiation. *J. Biomed. Mater. Res. Appl. Biomater.* 1997; 38: 289–300.
19. Aggrawal RK, Ireland DC, Azrin MA, Ezekowitz MD, Bono DPD, Gershlick AH. Antithrombotic potential of polymer-coated stents eluting platelet glycoprotein IIb/IIIa receptor antibody. *Circulation.* 1996; 94: 3311–3317.
20. Comel L. Aspetti fluidodinamici connessi alla restenosi coronarica. In: Graduate thesis, Dept. of Materials Engineering, Univ. Trieste, Italy, 2007.



## Modelling drug release in cardiovascular eluting stents

21. Acharya G, Park K. Mechanisms of controlled drug release from drug-eluting stents. *Adv. Drug Deliv. Rev.* 2006; 58: 387–401.
22. Russell ME. Comprehensive Review of the Polymer-Based Taxol Release Kinetics and Animal Data: Insights into Efficacy and Toxicity, 2002 Drug-Eluting Stent Summit@TCT 2002.
23. Leon MB, Abizaid A, Moses JW. The CYPHER Stent: A New Gold Standard in the Treatment of Coronary Artery Disease, The Cardiovascular Research Foundation, New York, 2003.
24. Finkelstein A, McClean D, Kar S, Takizawa K, Vargeese K, Baek N, Park K, Fishbein MC, Makkar R, Litvack F, Eigler NL. Local drug delivery via a coronary stent with programmable release pharmacokinetics. *Circulation.* 2003; 107: 777–784.
25. Nordmann AJ, Briel M, Bucher HC. Mortality in randomized controlled trials comparing drug-eluting vs. bare metal stents in coronary artery disease: a meta-analysis. *Euro. Heart J.* 2006; 27: 2784–2814.
26. Holmes DR Jr, Moses JW, Schofer J, Morice MC, Schampaert E, Leon MB. Cause of death with bare metal and sirolimus-eluting stents. *Euro. Heart J.* 2006; 27: 2815–2822.
27. Wijns WC, Krucoff MW. Increased mortality after implantation of first generation drug-eluting stents: seeing the smoke, where is the fire? *Euro. Heart J.* 2006; 27: 2737–2739.
28. Grassi G, Dawson P, Guarnieri G, Kandolf R, Grassi M. Therapeutic potential of hammerhead ribozymes in the treatment of hyper-proliferative diseases. *Curr. Pharm. Biotech.* 2004; 5(4): 369–386.
29. Khachigian LM, Fahmy RG, Zhang G, Bobryshev YV, Kaniaros A. c-Jun regulates vascular smooth muscle cell growth and neointima formation after arterial injury. Inhibition by a novel DNA enzyme targeting c-Jun. *J. Biol. Chem.* 2002; 277: 22985–22991.
30. Grassi G, Crevatin A, Farra R, Guarnieri G, Pascotto A, Rehimers B, Lapasin R, Grassi M. Rheological properties of aqueous pluronic-alginate systems containing liposomes. *J. Coll. Interf. Sci.* 2006; 301: 282–290.
31. Slepian MJ, Hubbell JA. Polymeric endoluminal gel paving: hydrogel systems for local barrier creation and site-specific drug delivery. *Adv. Drug Deliv. Rev.* 1997; 24: 11–30.
32. Eccleston DS, Lincoff AM. Catheter-based delivery for restenosis. *Adv. Drug Deliv. Rev.* 1997; 24: 31–43.
33. West JL, Hubbell JA. Separation of the arterial wall from blood contact using hydrogel barriers reduces intimal thickening after balloon injury in the rat: the roles of medial and luminal factors in arterial healing. *Proc. Natl. Acad. Sci. USA.* 1996; 93: 13188–13193.
34. Iavanova R, Lindman B, Alexandridis P. Evolution in Structural Polymorphism of Pluronic F127 Poly(ethylene oxide)-Poly(propylene oxide) Block Copolymer in Ternary Systems with Water and Pharmaceutically Acceptable Organic Solvents: From "Glycols" to "Oils". *Langmuir.* 2000; 16: 9058.
35. Strand BL, Mørch YA, Skjåk-Bræk G. Alginate as immobilisation matrix for cells. *Minerva Biotecnologica* 2000; 12: 223.
36. Grassi M, Grassi G, Lapasin R, I. Colombo I. Understanding drug release and absorption mechanisms: a physical and mathematical approach, CRC Press, Boca Raton (FL, USA), 1-627, 2007.
37. Pontrelli G, de Monte F. Mass diffusion through two-layer porous media: an application to the drug-eluting stent. *Int. J. Heat Mass Transf.* 2007; 50: 3658–3669.
38. Migliavacca F, Gervaso F, Prosi M, Zunino P, Minisini S, Formaggia L, Dubini G. Expansion and drug elution model of a coronary stent. *Comp. Meth. Biomech. Biomed. Eng.* 2007; 10(1): 63-73.
39. Yang C, Burt HM. Drug-eluting stents: factors governing local pharmacokinetics. *Adv. Drug Deliv. Rev.* 2006; 58: 402–411.
40. Creel C, Lovich M, Edelman E. Arterial paclitaxel distribution and deposition. *Circ. Res.* 2000; 86(8): 879–884.



CHAPTER 7 

41. Prosi M, Zunino P, Perktold K, Quarteroni A. Mathematical and numerical models for transfer of low-density lipoproteins through the arterial walls: a new methodology for the model set up with applications o the study of disturbed luminal flow. *J. Biomech.* 2005; 38: 903–917.
42. Kargol A, Kargol M, Przystalski S. The Kedem-Katchalsky equations as applied for describing substance transport across biological membranes. *Cell. & Molec. Biol. Letters* 1996; 2: 117–124.
43. Hwang C, Wu D, Edelman ER. Physiological transport forces govern drug distribution for stent-based delivery. *Circulation.* 2001; 104(5): 600–605.
44. Grassi M, Pontrelli G, Teresi L, Grassi G, Comel L, Ferluga A, Galasso L. Novel design of drug-eluting stents: the influence of hemodynamics and mass release, submitted, 2007.

